

P. Amaudruz¹, D. Bryman², L. Kurchaninov¹, P. Lu³, C. Marshall¹, J. P. Martin³, A. Muennich¹, F. Retiere¹, A. Sher¹
¹TRIUMF, 4004 Wesbrook Mall, Vancouver, BC, V6T 2A3
²University of British Columbia, 2329 West Mall Vancouver, BC Canada V6T 1Z4
³University of Montreal, Montreal, PQ, Canada

Introduction

This work is aimed at studying the interactions of 511 keV photons in liquid xenon (LXe) detectors for applications to positron emission tomography (PET). The advantages of LXe for PET compared to crystals include improved energy resolution, sub-mm spatial resolution, and larger detector volumes with high sensitivity. Figure 1 shows the concept of a LXe microPET scanner. Using a small test chamber we measured scintillation light and ionization charge signals in order to study the energy resolution in LXe.

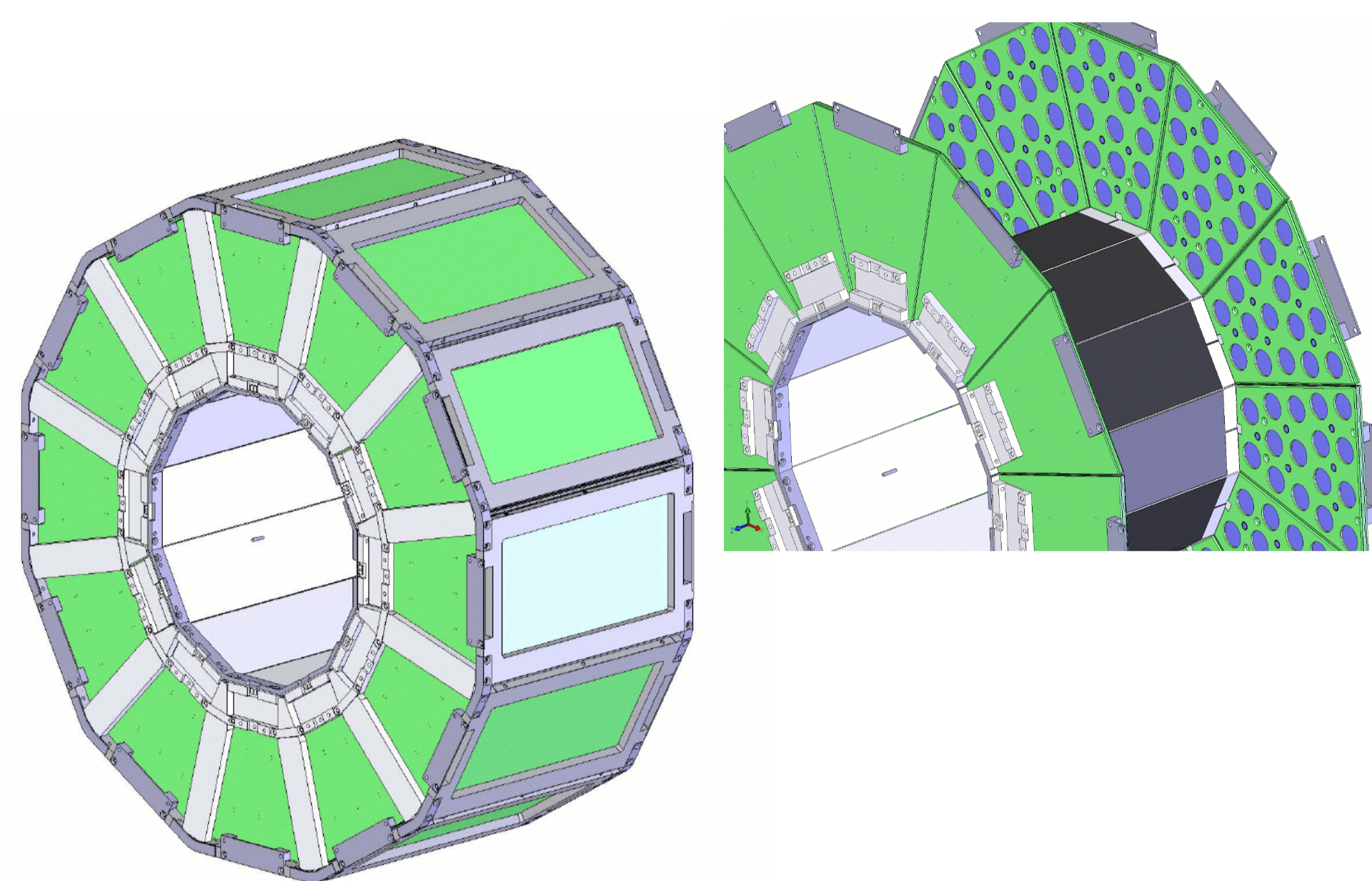


Figure 1. The LXe PET ring concept. Scintillation light and charge are measured in each of the 12 modules consisting of a LXe time projection chamber viewed by avalanche photodiodes.

The Test Chamber

A small test chamber (27 cm³) was constructed to measure light and charge signals. An electric drift field was applied between the cathode and the shielding grid located near the anode charge collection plane as shown in fig. 2. Two large area avalanche photodiodes (LAAPD from API) were used to detect the scintillation light. Charge was collected on a central 1 cm dia. electrode (A1) or on an outer electrode (A2). The 511 keV photons emitted by a ²²Na source entered the test chamber (along the z axis) through the cathode plane and coincidences with an external NaI detector were studied.

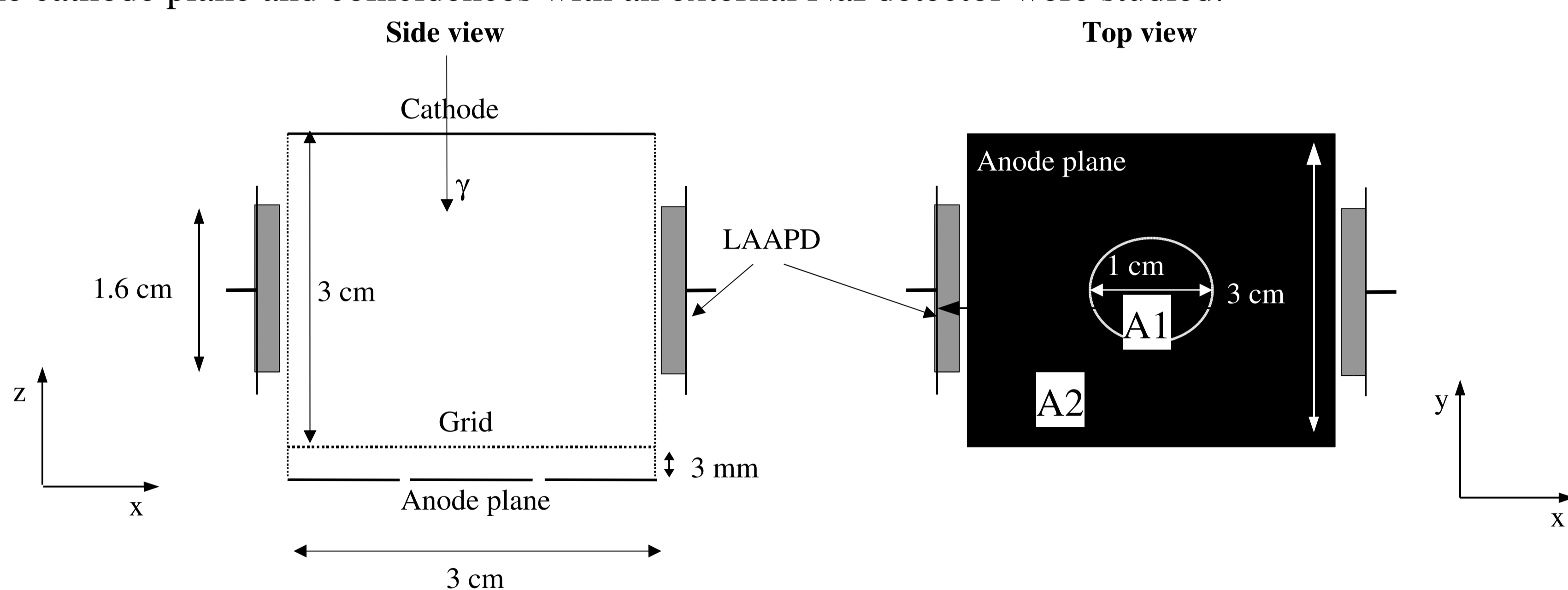


Figure 2. Side and top views of the test chamber.

Charge and Light Collection

Table 1 below gives results for charge and light collection at different drift fields for 511 keV photons. Photoelectric peak events and Compton scattering interactions were observed as shown in fig. 3. From the observed charge distributions, the drift velocity, total charge, and the charge attenuation length (or electron drift lifetime) were measured. From the light distribution the total number of photons observed and also the charge drift velocity were obtained. The spatial resolution (rms) in the drift direction using only the observed light amplitude of the two LAAPDs for photo-peak events was 3 mm; the spatial resolution from charge measurements is expected to be approximately 0.3 mm in all three dimensions.

E_d [kV/cm]	v_d [cm/ μ s]	Q_{tot} (e ⁻) _(511keV)	N_{tot} (γ) _(511keV)
0.33	0.15 \pm 0.01	16,000 \pm 2,000	16,500 \pm 2,000
1	0.17 \pm 0.01	19,000 \pm 2,000	14,500 \pm 2,000
2	0.20 \pm 0.01	21,000 \pm 2,000	13,500 \pm 2,000

Table 1: Electric field (E_d), drift velocity (v_d), and numbers of e⁻ (Q_{tot}) and photons (N_{tot}) observed.

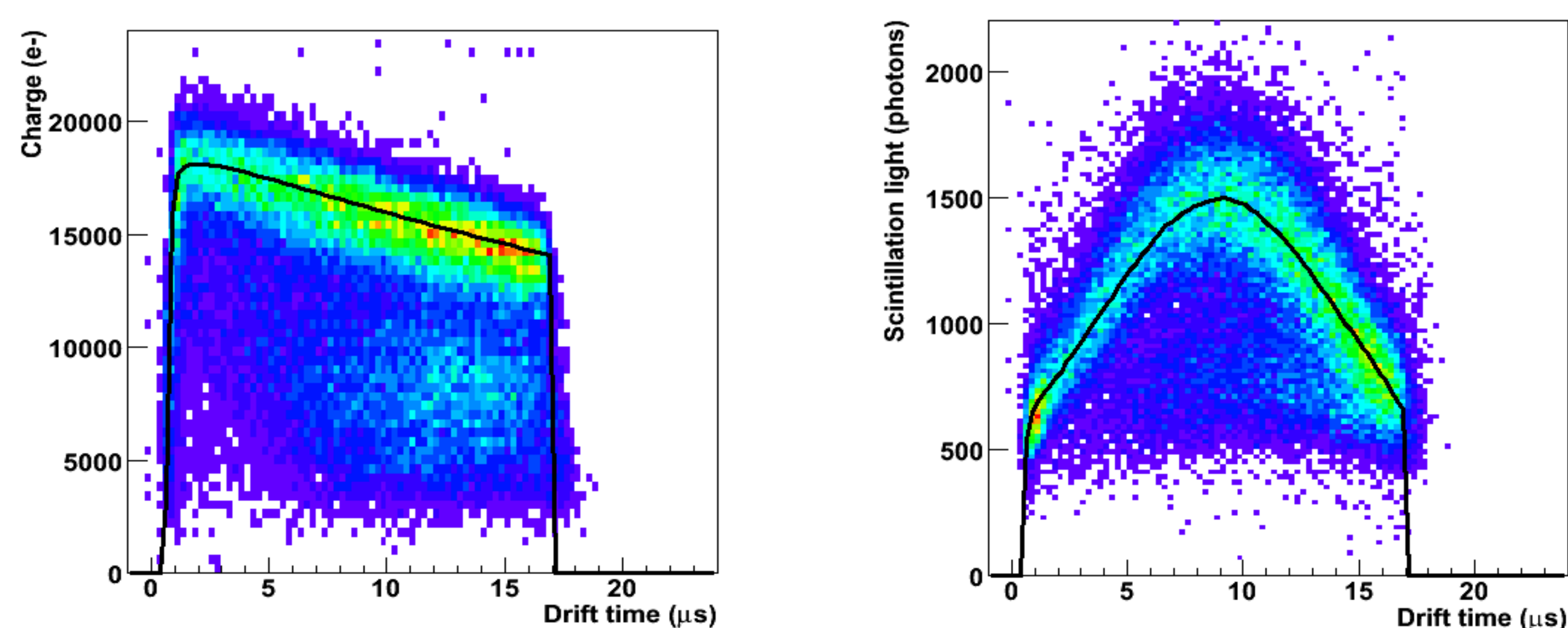


Figure 3. Charge (left) and light (right) collection as a function of drift time for a 1 kV/cm drift field. The curves are fits based on parameterizations obtained from current calculations and solid angle.

Energy Resolution

To study the energy resolution we focused on the central region of the test chamber (A1 at z=1.5 cm from the cathode). Figure 4 shows the energy distributions observed for charge, light and the combination of both. The 511 keV region ellipse of the charge-light anti-correlation was fit and projected along the ellipse axis. Combining the information of the light and charge measurements, energy resolution (rms) as low as 3.78% was achieved as given in Table 2. An analysis of the contributing sources of errors is given in the Appendix below.

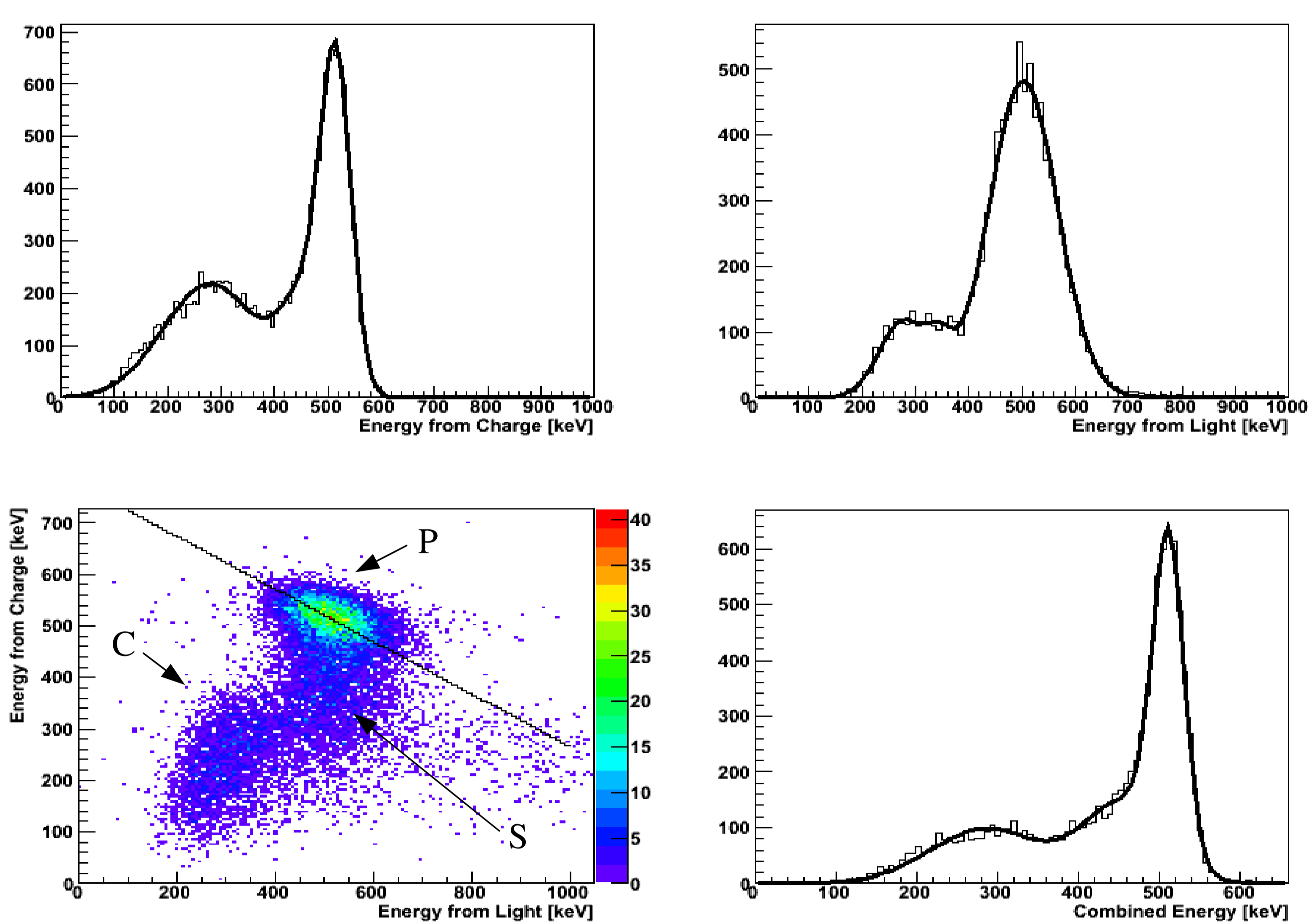


Figure 4. The observed charge spectrum (upper left plot), light spectrum (upper right plot), correlation between light and charge signals (lower left plot), and combined spectrum using the correlation (lower right plot) for 511 keV photons with a drift field of 2.66 kV/cm. The data points in the correlation plot that are not part of the Compton (C) or the photoelectric peak (P) are due to photons that scattered outside the detector (S).

Drift Field [kV/cm]	0.33	1	2	2.66
Energy Resolution (charge) [%]	9.21 \pm 0.38	5.38 \pm 1.04	5.69 \pm 0.29	4.78 \pm 0.16
Energy Resolution (light) [%]	13.90 \pm 0.19	12.39 \pm 0.32	12.41 \pm 0.28	12.73 \pm 0.16
Energy Resolution (combined) [%]	4.70 \pm 0.11	4.30 \pm 0.22	4.54 \pm 0.12	3.78 \pm 0.09

Table 2: Energy resolutions (rms) observed at different drift fields.

Summary of Results with the LXe Test Chamber

- Electron lifetime: > 200 μ s
- Time resolution: 1 ns
- Energy resolution: <4%
- Spatial resolution obtainable from charge (light): 0.3 (3) mm

Future Work

A complete single sector for a PET ring is under construction. This will be followed by coincidence measurements using two or more sectors.

Appendix: Energy Measurement Error Analysis

- **Light resolution**
 - Electronics noise (2%)
 - APD gain (3%)
 - Light-position fluctuation (3%)
 - Light-charge fluctuation (12%)
$$\left(\frac{\Delta S m}{S m}\right)^2 = \left(\frac{ENC_s}{M S m}\right)^2 + \frac{D(M)}{M^2 S m} + \left(\frac{\Delta F_\Omega}{F_\Omega}\right)^2 + \left(\frac{Q_i \Delta F_r}{S_i + Q_i F_r}\right)^2$$
- **Charge resolution**
 - Electronics noise (2%)
 - Light-charge fluctuation (5%)
$$\left(\frac{\Delta Q m}{Q m}\right)^2 = \left(\frac{ENC_q}{Q m}\right)^2 + \left(\frac{\Delta F_r}{1 - F_r}\right)^2$$
- **Light-charge combined resolution**
 - Light resolution (4%)
 - Charge resolution (2%)
$$\left(\frac{\Delta E c}{E c}\right)^2 = \left(\frac{ENC_s}{M S m}\right)^2 + \frac{D(M)}{M^2 S m} + \left(\frac{\Delta F_\Omega}{F_\Omega}\right)^2 + \left(\frac{ENC_q}{Q m}\right)^2$$